

THE SIGNIFICANCE OF AERODYNAMIC JET INTERFERENCE IN
DEVELOPMENT AND TESTING OF THE DO 31 V/STOL TRANSPORT -

D. Welte

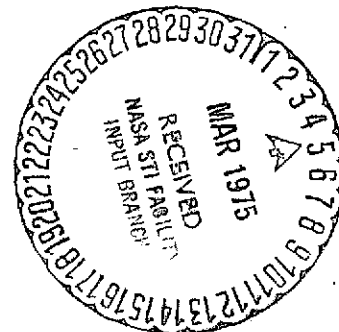
(NASA-TT-F-16165) THE SIGNIFICANCE OF
AERODYNAMIC JET INTERFERENCE IN DEVELOPMENT
AND TESTING OF THE DO 31 V/STOL TRANSPORT
(Kanner (Leo) Associates) 25 p HC \$3.25

N75-17335

Unclas

CSCL G1C G3/05 10260

Translation of "Die Bedeutung der aerodynamischen Strahl-
interferenz bei der Entwicklung und Erprobung des V/STOL-
Transportflugzeuges Do 31," Deutsche Gesellschaft fur Luft-
und Raumfahrt, Jahrestagung, 5th, Berlin, West Germany,
Oct. 4-6, 1972, Paper 72-106



STANDARD TITLE PAGE

1. Report No. NASA TT F-16,165	2. Government Accession No.	3. Recipient's Catalog No.	
4. Title and Subtitle THE SIGNIFICANCE OF AERO-DYNAMIC JET INTERFERENCE IN DEVELOPMENT AND TESTING OF THE DO 31 V/STOL TRANSPORT		5. Report Date February 1975	
		6. Performing Organization Code	
7. Author(s) D. Welte, Dornier Corporation		8. Performing Organization Report No.	
		10. Work Unit No.	
9. Performing Organization Name and Address Leo Kanner Associates Redwood City, California 94063		11. Contract or Grant No. NASW-2481	
		13. Type of Report and Period Covered Translation	
12. Sponsoring Agency Name and Address National Aeronautics and Space Administration, Washington, D.C. 20546		14. Sponsoring Agency Code	
15. Supplementary Notes Translation of "Die Bedeutung der aerodynamischen Strahlinterferenz bei der Entwicklung und Erprobung des V/STOL-Transportflugzeuges Do 31," Deutsche Gesellschaft für Luft- und Raumfahrt, Jahrestagung, 5th, Berlin, West Germany, Oct. 4-6, 1972, Paper 72-106			
16. Abstract Model measurements performed in the wind tunnel indicated a 3.5% lift loss during hover, increasing to 7 or 8% close to the ground. During transition, the jet-induced, tail-heavy moment demanded a large part of available trimming moment. A series of VTOL transitions flown by the Do 31 E3 test aircraft has been analyzed with regard to jet-induced forces and moments. Agreement between model and flight measurements is satisfactory, supporting the model engineering and model laws. A familiar, simple, semiempirical method for calculating jet-induced normal force during hover is extended to complex configurations such as that of the Do 31.			
17. Key Words (Selected by Author(s))		18. Distribution Statement Unclassified-Unlimited	
19. Security Classif. (of this report) Unclassified	20. Security Classif. (of this page) Unclassified	21. No. of Pages 20	22. Price

Table of Contents

	<u>Page</u>
1. Summary	1
2. The Do 31	2
3. The Pattern of Flow	2
4. Jet Interference during Do 31 Development	3
4.1. The Wind Tunnel Model	3
4.2. Measurement Results	4
5. Jet Interference during Do 31 Testing	6
5.1. Data Acquisition and Preparation	6
5.2. Jet Interference Measurements	7
6. Calculation of Jet-Induced Normal Force in Hover	9
References	20

List of Figures

- Fig. 1. DDoe31 power plant and control system.
- Fig. 2. Do 31 flow field during vertical takeoff.
- Fig. 3. Do 31 jet interference model in wind tunnel.
- Fig. 4. Jet interference in Do 31 hover close to ground -- wind tunnel measurements.
- Fig. 5. Jet interference~~in~~ in Do 31 transition out of ground effect -- wind tunnel measurements.
- Fig. 6. Do 31-E3 V/STOL transport.
- Fig. 7. Pitch trimming moment curves for a series of Do 31 VTOL transitions.
- Fig. 8. Jet interference in a Do 31-E3 landing transition and comparison with wind tunnel measurements.
- Fig. 9. Jet interference due to ground effect in three Do 31 vertical landings.
- Fig. 10. Expression for calculating jet interference in hover.

Notation

b	Wingspan
D_a	Nozzle diameter
F	Thrust
h	Altitude (distance between landing gear and ground)
K	Constant
l_μ	Mean aerodynamic chord
L	Rolling moment
M	Pitching moment (positive if tail-heavy)
N	Normal force (positive if upward in normal attitude)
P_o	Total pressure in nozzle
P_∞	Ambient static pressure
$q(x)$	Stagnation pressure along axis of jet
r	Polar coordinate (see Fig. 10)
S	Reference wing area
S_a	Nozzle area
V_∞	Airspeed
w_a	Jet exhaust velocity
θ	Pitch angle
θ	Roll angle
σ	Thrust setting angle ($\sigma = 0$: forward thrust; $\sigma = 90^\circ$: upward thrust)
ϕ	Polar coordinate (see Fig. 10)
ϕ	Roll angle

THE SIGNIFICANCE OF AERODYNAMIC JET INTERFERENCE IN
DEVELOPMENT AND TESTING OF THE DO 31 V/STOL TRANSPORT

D. Welte,
Dornier Corporation

1. Summary

/1*

Aerodynamic jet interference, i.e. power plant jet feedback effects on aircraft aerodynamics, primarily reduces maximum permissible vertical takeoff weight and pitch control reserve during Do 31 transition. Jet-induced forces and moment are largely determined experimentally.

Model measurements performed in the wind tunnel indicated a 3.5% lift loss during hover, increasing to 7 or 8% close to the ground. During transition, the jet-induced, tail-heavy moment demanded a large part of available trimming moment.

A series of VTOL transitions flown by the Do 31 E3 test aircraft has been analyzed with regard to jet-induced forces and moments. An extensive data acquisition and evaluation system was available for this purpose. The required measurement precision could not be achieved in all cases. Nevertheless, agreement between model and flight measurements is satisfactory, supporting the model engineering and model laws.

A familiar, simple, semiempirical method for calculating jet-induced normal force during hover is extended to complex configurations such as that of the Do 31.

* Numbers in the margin indicate pagination in the foreign text.

2. The Do 31

/4

The Do 31 is a jet-supported VTOL transport aircraft. The power plant and control system is shown in Fig. 1. Four lift power plants are housed in pods at each of the wing tips. They are installed at an angle of $\sigma = 75^\circ$ relative to the horizontal (thrust vector upward and forward). The cruising power plants are suspended inboard under the wing and have four pivoting nozzles each (pivoting range $10^\circ < \sigma < 120^\circ$), which are used for thrust support during hover and for acceleration and braking during transition. The ratio of lift thrust to cruising thrust is about 1.3.

Control about the pitch axis is achieved with air tapped from the cruising power plants, discharged via two control nozzles mounted at the tail. Control about the roll axis is achieved through opposite changes in thrust at the power plant pods and about the yaw axis through opposite pivoting of the lift power plant nozzles. Aerodynamic control is conventional.

3. The Pattern of Flow

Aerodynamic jet interference, or jet interference for short, refers to the indirect action of the power plant jets on aircraft aerodynamics. Jet interference affects the balance of forces and moments and must be taken into consideration back in the initial stages of aircraft design.

In hover close to the ground, the jet effect is based on three factors (Fig. 2): The sinking effect results from turbulent jet mixing with surrounding air and produces an underpressure on the underside of the aircraft. High-energy exhaust fountains flow against the underside of the aircraft between neighboring power plants or groups of power plants and produce an upward-directed force. Power plant jets which exhaust downward between

/5

the ground and underside of the aircraft at high velocity produce a suction effect. The three effects overlap in quite different ways in different cases.

In hover outside of the ground effect, only the sinking effect is operant. Three other effects are added to this in flight. The blockage of flow about the aircraft by the presence of the power plant jets produces a local change in pressure distribution. Reduced total pressure exists in the jet wake. A downwash is induced by jet deflection in the direction of oncoming flow. Overall all, jet interference produces a lift loss and a tail-heavy moment during Do 31 transition.

4. Jet Interference during Do 31 Development

A theoretical treatment of jet interference was not possible for the Do 31. Jet-induced normal force can be estimated semi-empirically only for the relatively simple case of hover outside ground effect. This is covered in Section 6. The jet-induced forces and moments required for flight-mechanics calculations were determined with model measurements taken in the wind tunnel.

4.1. The Wind Tunnel Model

/6

The jet interference model of the Do 31, scale 1:20, is shown in Fig. 3. The model is suspended with the balance cables in the Dornier wind tunnel ($2.2 \times 3.2 \text{ m}^2$). To simulate the power plant jets, compressed air is discharged from three nozzles each in the lift and cruising power plant wing pods on each side. The nozzles and air lines are suspended so as not to make contact with the model. Power plant thrust is determined from flow conditions upstream from the nozzles. A ground panel, adjustable in height and inclination, is used to simulate the ground. The power plant inlets are not simulated.

The following parameters can be adjusted to simulate VTOL transitions:

Ratio of momentum densities for cruising power plant thrust, lift power plant thrust and oncoming flow:	$I_{CPP}/I_{LPP}/I_{\infty}$
Thrust setting of cruising power plants:	σ
Ground distance:	h/b
Pitch angle and roll angle:	θ, ϕ
Angle of attack:	α

The jet-induced forces and moments are obtained from six-component measurements, as the difference between measurements made with and without thrust.

4.2. Measurement Results

17

Fig. 4 shows jet interference (lift loss, pitching moment and rolling moment) in hover close to the ground and at a higher altitude. In hover out of ground effect, lift loss is between 3 and 4% of total thrust, whereas it increases to 7.5% close to the ground. In case of cruising power plant failure, lift loss decreases to 2 to 3% in hover out of ground effect, since the lift power plants mounted on the wing tips contribute less than the cruising power plants mounted inboard under the wing. The latter case is decisive for maximum vertical takeoff weight.

If we set thrust equal to weight, as during landing, jet-induced pitching moment out of ground effects can be looked upon as a 1.8% forward shift in the aft-most controllable center of gravity position. Close to the ground, the jet-induced pitching moment has a stabilizing effect. At $\theta = 0^\circ$, it produces a 3.5% aftward shift in the forward-most controllable center of gravity position. Thus jet interference reduces the controllable center of gravity range in hover by 5.3%. In practice, however, no

limitations were encountered during vertical takeoff and during vertical landing, since the large nose-heavy change in moment is operant only to a ground distance of about 1 m and thus acts for only a second or so. For a moment of inertia of 30,000 mkg/s² about the pitch axis, this disturbance would cause a rotation of about 3°.

Jet-induced rolling moment has a destabilizing effect. In an extremely tilted attitude, rolling moment corresponds to a lever arm for total thrust of 2.5% of one-half span, as opposed to the maximum available control moment of 17%.

Fig. 5 shows aerodynamic jet interference in transition. Jet- /8 induced normal force and pitching moment are plotted over effective velocity ratio

$$\left(\frac{V_\infty}{w_a} \right)_{\text{eff}} = \sqrt{\frac{V_\infty^2 \sin \alpha}{w_a^2 \sin \alpha_0}}$$

where $(V_\infty/w_a)_{\text{eff}}$ corresponds to the ratio of momentum densities of oncoming flow and power plant thrust and serves as a characteristic quantity for converting from model to full scale. Jet interference increases with aircraft speed. As in hover, the interference effect of the cruising power plants predominates. This is shown clearly in the Figure by the pronounced effect of thrust angle. Measurements made without the elevator show that about half of the jet-induced pitching moment is applied to the elevator.

Typical thrust angles during takeoff and landing transitions are shown in the Figure. In takeoff transition, cruising power plant thrust is turned forward rather quickly, so interference remains low. During almost the entire landing transition, however, cruising power plant thrust is directed upward or even upward and aftward, as a result of which jet-induced pitching moment at 150 knots approaches the maximum jet control moment of

$\Delta M/F \times l_{\mu} = 0.125$. Total pitch control moment in transition is made up of jet control moment and aerodynamic moment. In the least favorable case, almost the entire pitch control moment is required for trimming (aerodynamic + jet-induced). The least favorable case occurs in flight at an angle of attack of -10 to -12° with the aft-most center of gravity position.

The conclusion drawn for flight tests was the advisability of flying with a positive angle of attack in transition, if feasible.

5. Jet Interference during Do 31 Testing

/9

5.1. Data Acquisition and Preparation

Jet-induced normal force and pitching moment were determined from the balance of forces and moments for a series of VTOL transitions by the Do 31 E3 test aircraft. Fig. 6 shows this aircraft. Of the measured values stored onboard on magnetic tape, 120 were to be processed just for jet interference evaluation. Data were recorded at a frequency of 5 Hz or more.

Instantaneous gross weight was determined from takeoff weight, fuel consumption and normal acceleration. The rpm method was used to determine thrust for the eight lift and two cruising power plants, based on the applicable static-operation data supplied by the engine manufacturers. Flight variables were measured with the Dornier Fluglog and the Pitot tube. Conventional aerodynamic coefficients and derivatives were obtained partly from wind tunnel measurements and partly from flight tests with the Do 31 E1 test aircraft provided for conventional flight testing. The E1 differed from the E3 in the absent intake flaps, intake cascades and spreading exhaust flaps on the lift power plant pods. For this reason, it was necessary to correct the zero momentum coefficient by $\Delta c_{M_0} = -0.067$, obtained by evaluating the balance of moments in the conventional flight phase of the E3.

The data taken in each measurement exhibit a dispersion; outliers are also possible. Most of the 120 measured data were therefore subjected to a smoothing process. A third-degree polynomial was used whose coefficients were determined by the method of least squares. It proved desirable to extend the smoothing range per data point over 15 neighboring values each, corresponding to 3 msec each before and after the data point. Weighting was based on Gauss' error function. /10

Jet-induced normal force and pitching moment are obtained as differences between several large numbers. Data imprecisions of a few percent have pronounced effects on the results. Instantaneous gross weight could be determined to less than 1%. On the other hand, thrust determination involved an error of $\pm 3\%$. This can be seen from a comparison between the thrust balances for different hovers. The error in thrust determination is eliminated by taking the hover condition out of ground effect as the zero point and considering only the change in normal force and in pitching moment with aircraft speed at ground distance. Since the level of power plant thrust was high and approximately constant in the Do 31 E3 VTOL transitions evaluated, rpm-dependent errors which may occur in thrust determination are not appreciable.

5.2. Jet Interference Measurements

It was learned from the jet interference measurements made in the wind tunnel that considerable tail-heavy jet-induced moments can be expected during Do 31 VTOL transitions. Flight tests support this prediction. Fig. 7 shows the curves of required pitch trimming moments versus aircraft speed in two takeoff and two landing transitions flown with the Do 31 E3. Transition time was supposed to be shortened in VTO transition No. 72. It was necessary to fly at the largest possible negative angle of attack for this, since lift power plant thrust then contributes to forward /11

acceleration. The actual angle of attack in takeoff transition 72 was between -5 and -11° . In VL transition 67, mean angle of attack was 0° . The smaller the angle of attack, the more control moment required for aerodynamic trimming, so in an extreme case such as takeoff transition 72, almost all available control moment must be applied to trimming. For this reason, the transition procedure used in all later flights was modified so that only positive angles of attack occurred (VL No. 238 and VTO No. 248).

Jet-induced normal force and pitching moment were calculated for a series of VTOL transitions by the measurement and evaluation method described. Fig 8 shows the effect of aircraft speed during landing transition. As mentioned, the reference state is hover outside ground effect. At an aircraft speed of about 100 knots, descent begins with a path angle of about 8° and a pitch angle of about -6° . The lift and cruising power plants operate at about 80% takeoff thrust, and the cruising power plant thrust angle is 108° , causing aircraft speed to be reduced. Flattening-out begins at about 30 knots, and the remaining slowdown is completed by increasing pitch angle and rotating cruising power plant thrust to 93° . Curves from the wind tunnel measurements are drawn in for comparison. Fig. 9 shows the effect of ground distance during three vertical landings and the corresponding wind tunnel curves. During an almost vertical descent, pitch angle is 6° until just before touchdown, and cruising power plant thrust setting is 94° . Here, too, the reference state is hover out of ground effect.

Agreement between wind tunnel measurement and flight test is satisfactory if we consider that the average difference is 1.5% of thrust for normal force, or corresponds to a shift in the point of thrust application by 1.5% of reference chord length for pitching moment.

/12

6. Calculation of Jet-Induced Normal Force in Hover

Systematic model measurements by NASA [1,2] with fighter configurations resulted in an empirical relationship between jet-induced lift loss in hover, aircraft size and jet characteristics (Fig. 10). For the configurations studied there, with a primarily central arrangement of jets, the constant has a value of $K = 0.009$. The value of K probably changes for a peripheral arrangement of power plant jets. Jet-induced lift loss would have to decrease particularly for lift powerplants mounted outboard on the wing, since a relatively small wing area exists in the immediate vicinity of the jets. In fact, the four lift power plants installed in a pod at the wing tip caused a 2.2% lift loss in the Do 31, whereas the lift loss for the four cruising power plant nozzles located inboard under the wing was 3.6%. Jet area was approximately the same in both cases here, as were jet characteristics.

The effect of the different distribution of aircraft area surrounding the jet is meant to be taken into consideration by replacing the area ratio with the following expression in the relationship given with Fig. 10:

$$\sqrt{\frac{S}{S_0}} = \frac{\int_0^{2\pi} |r(\varphi) - \frac{1}{2} D_0| d\varphi}{\pi D_0} \quad (1)$$

This expression covers the physically reasonable assumption that jet induction decreases with the reciprocal of distance from the jet axis. Two examples for the Do 31, with lift power plants only in operation and with cruising power plants only in operation, are used for calculations with the old and new expressions, which are compared with model measurements. Since the drop in stagnation pressure in the jet was not known from the Do 31 model measurements, values from [1] for standard nozzles in a group of four /13

were used for both examples. The calculations were carried out for each individual jet and the results superimposed linearly. Results of the calculations and of the wind tunnel measurements are given in the table below.

		$\Delta N/F$	
		Lift power plant	Cruising power plant
Calculation	From [1]	0.04	0.039
Calculated	From Eq. (1)	0.024	0.034
Model measurements		0.022	0.036

Both the old and the new expressions come quite close to the measured values for the cruising power plants, whereas for the lift power plants, this applies only to the new expression. This result is reasonable, since an extreme boundary condition occurs in the case of the lift power plants, in which the considerations which produced the new expression come to bear completely.

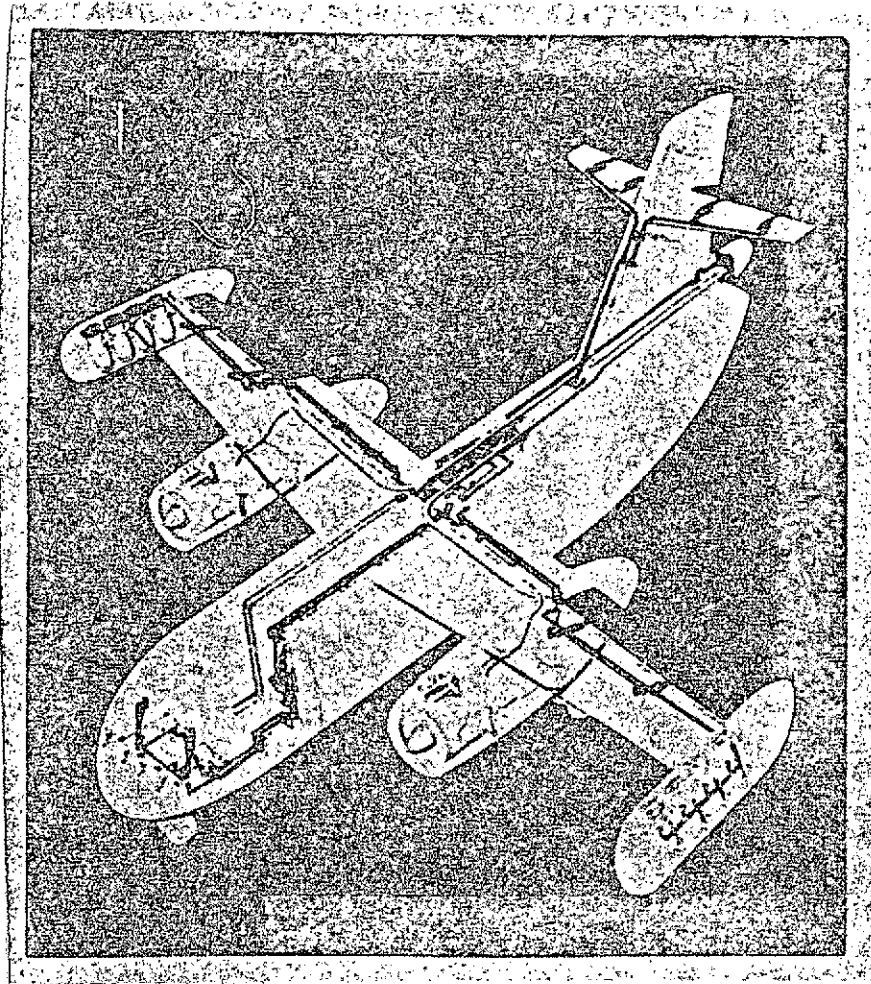


Fig. 1. Do 31 power plant and control system.

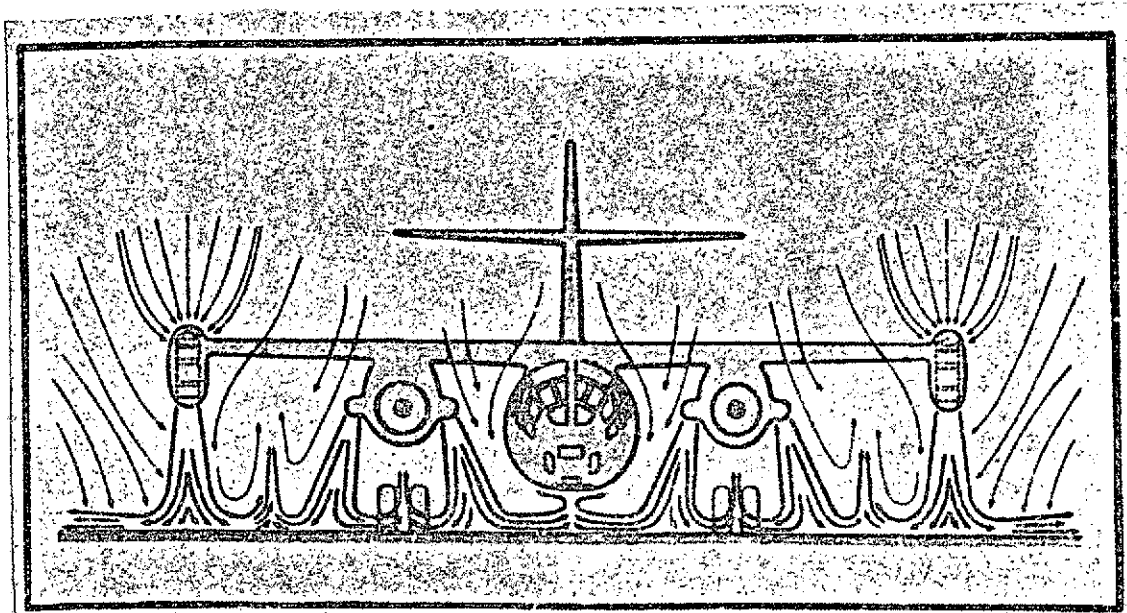


Fig. 2. Do 31 flow field during vertical takeoff.

ORIGINAL PAGE IS
OF POOR QUALITY

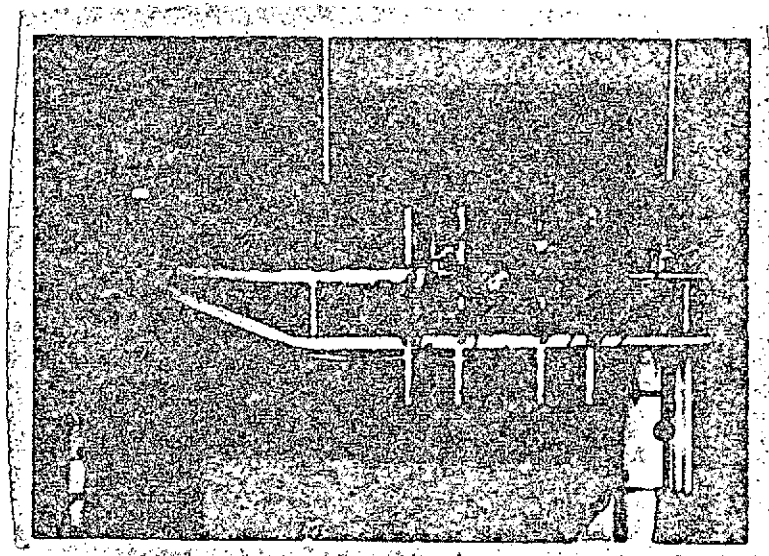


Fig. 3. Do 31 jet interference model in wind tunnel.
Measurement parameters:

Momentum ratio	$I_{CPP}/I_{LPP}/I_{\infty}$
Thrust angle	σ_{CPP}
Ground distance	h/b
Angle of pitch	θ
Angle of roll	ϕ
Angle of attack	α

ORIGINAL PAGE IS
OF POOR QUALITY

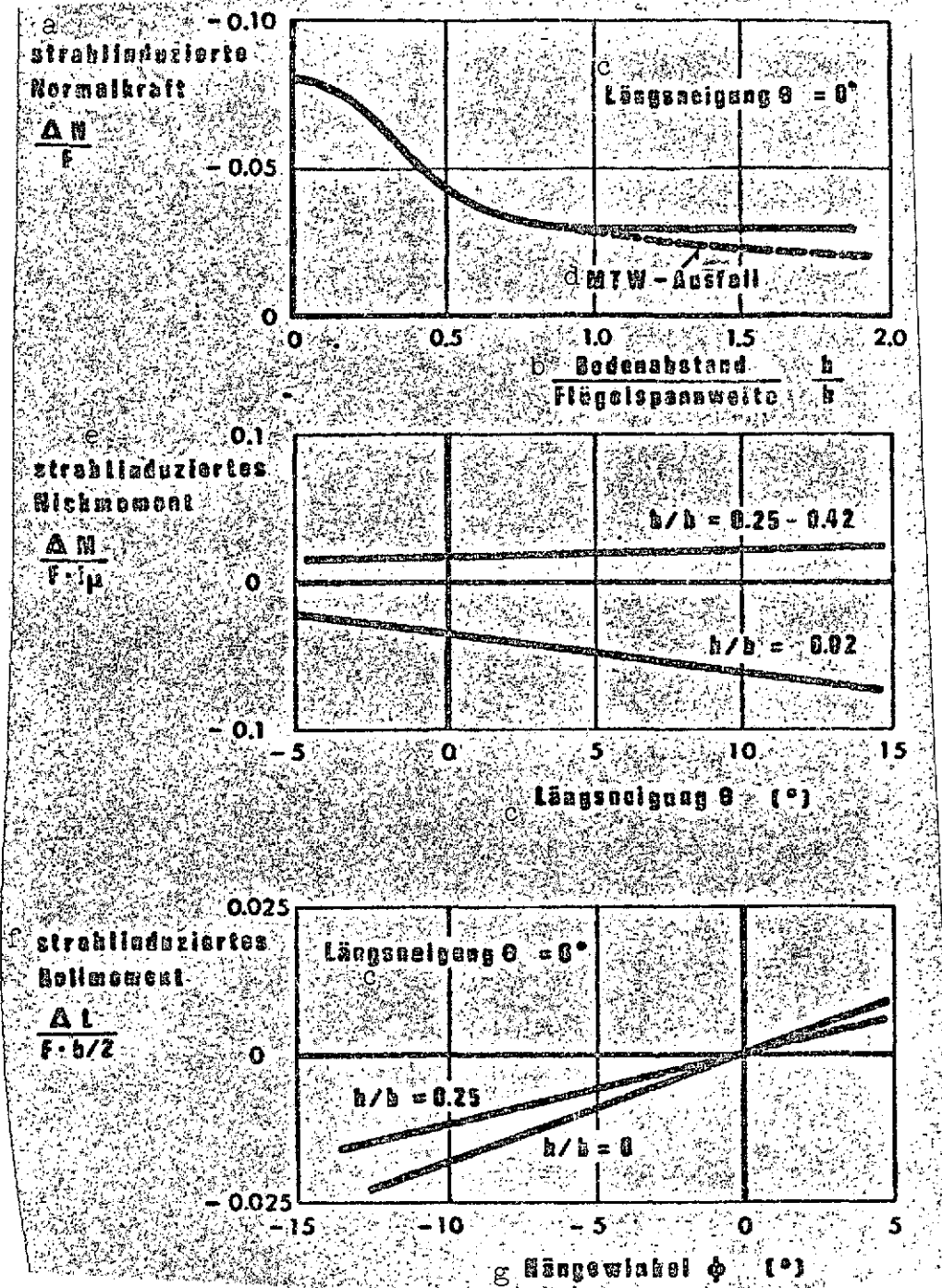


Fig. 4. Jet interference in Do 31 hover close to the ground -- wind tunnel measurements.

Key: a. Jet-induced normal force; b. Ground distance / wingspan; c. Angle of pitch; d. Cruising power plant failure; e. Jet-induced pitching moment; f. Jet-induced rolling moment; g. Angle of roll

ORIGINAL PAGE IS
OF POOR QUALITY

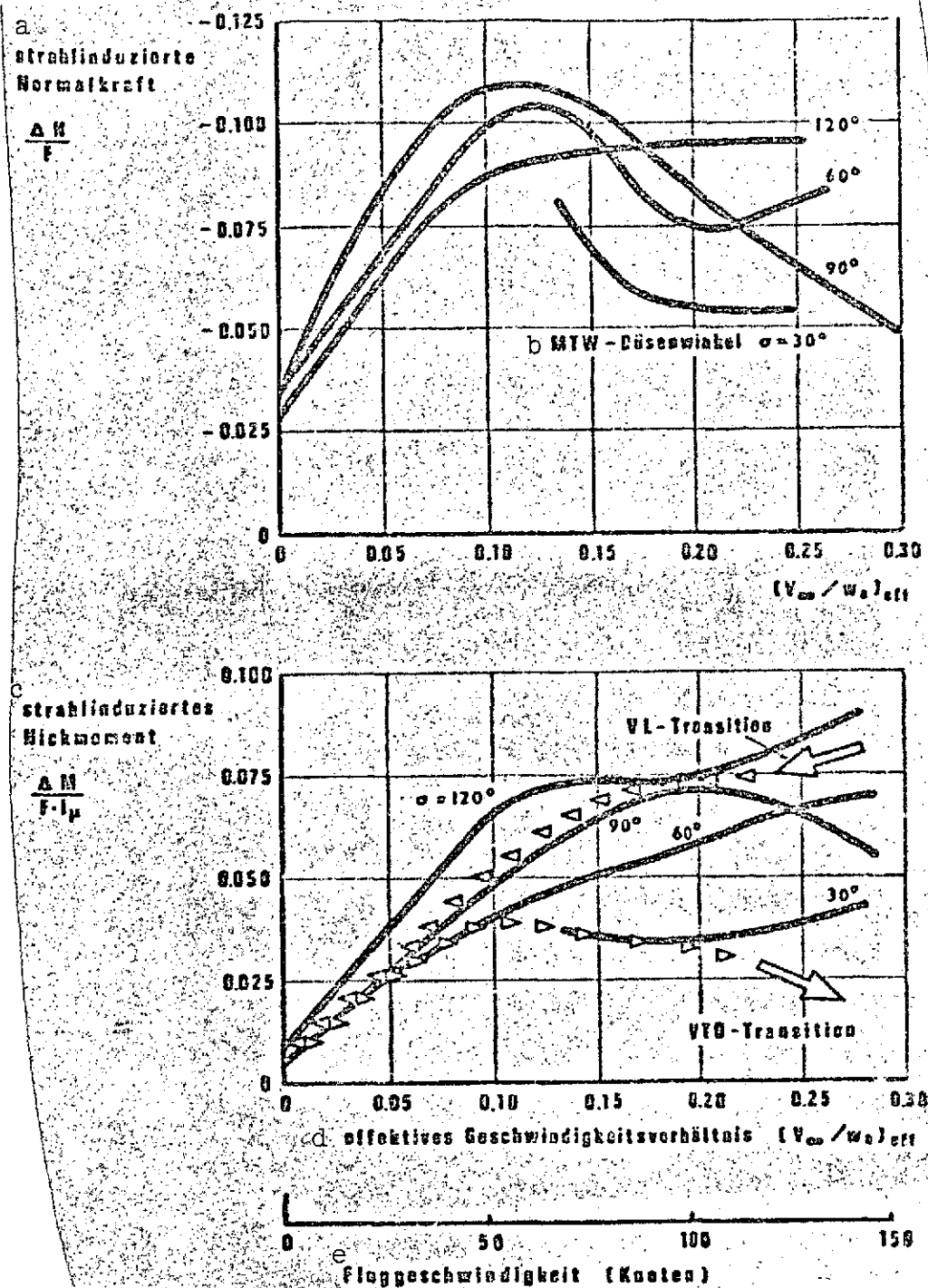


Fig. 5. Jet interference in Do 31 transition out of ground effect
 -- wind tunnel measurements.

Key: a. Jet-induced normal force; b. Cruising power plant nozzle angle; c. Jet-induced pitching moment; d. Effective velocity ratio; e. Airspeed (knots)

ORIGINAL PAGE IS
 OF POOR QUALITY

ORIGINAL PAGE IS
OF POOR QUALITY

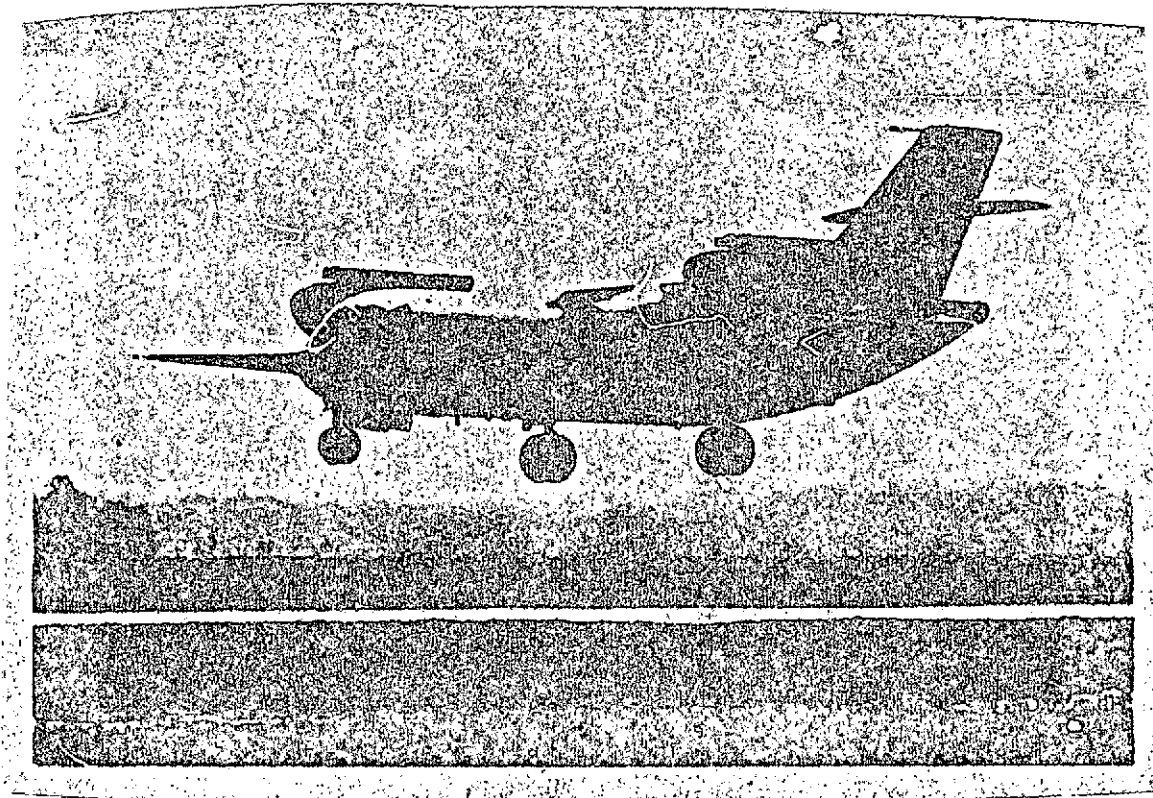


Fig. 6. Do 31-E3 V/STOL transport.

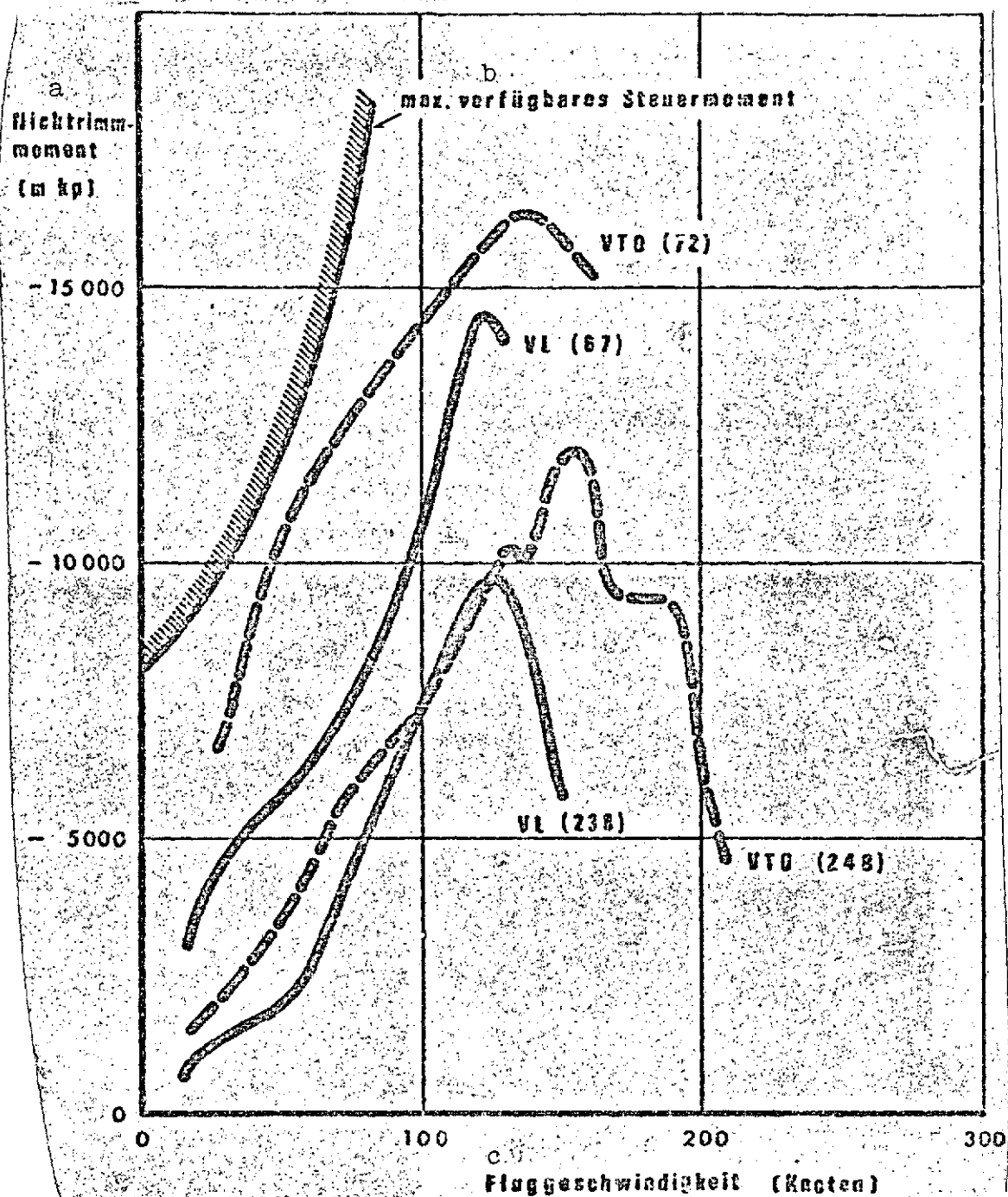


Fig. 7. Pitch trimming moment curves for a series of Do 31 VTOL transitions.

Key: a. Pitch trimming moment; b. Maximum available control moment; c. Airspeed (knots)

ORIGINAL PAGE IS
OF POOR QUALITY

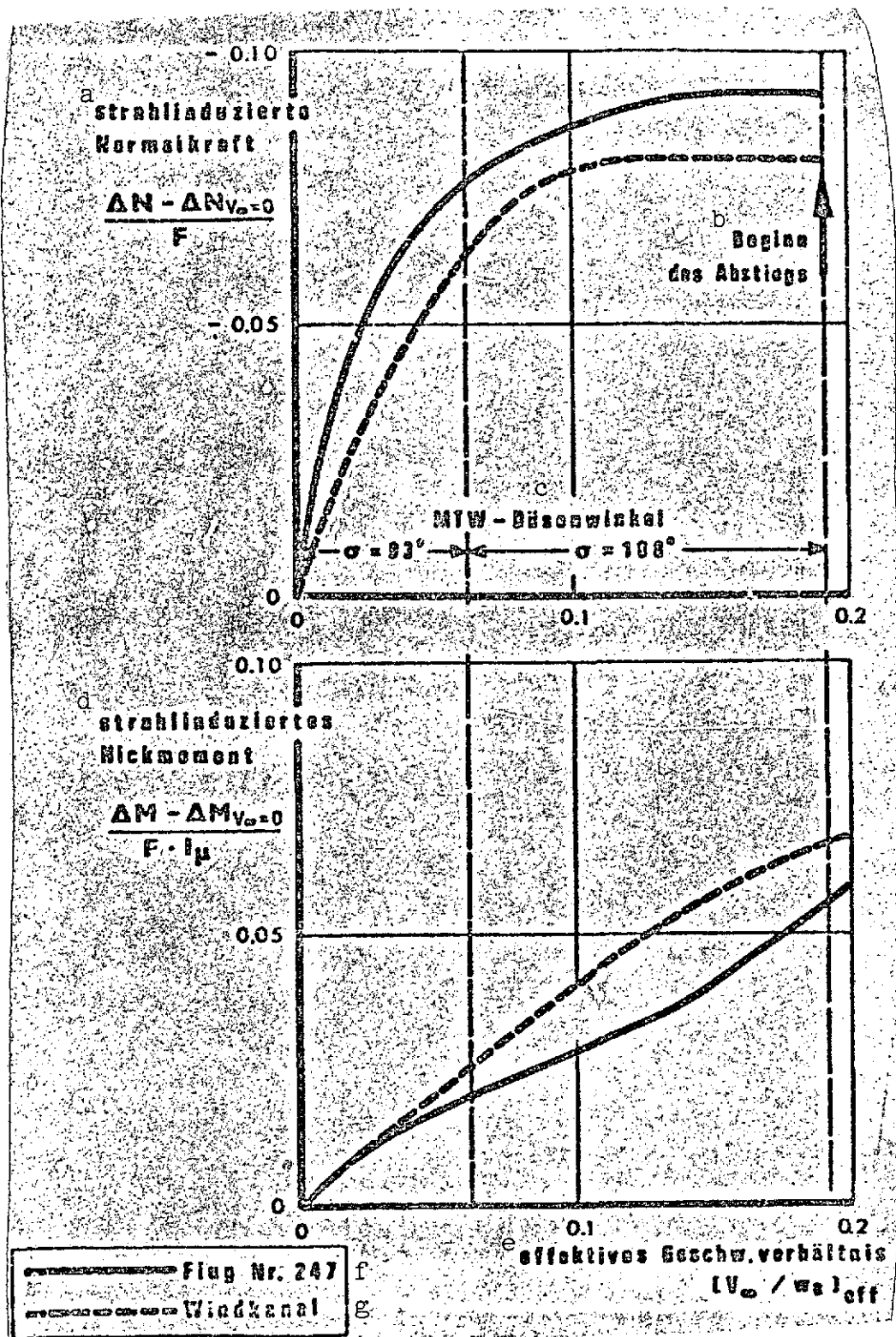


Fig. 8. Jet interference in a Do 31-E3 landing transition and comparison with wind tunnel measurements.

Key: a. Jet-induced normal force; b. Beginning of descent; c. su
cruising power plant nozzle angle; e. Jet-induced pitching mo-
ment; e. Effective velocity ratio; f. Flight 247; g. Wind
tunnel

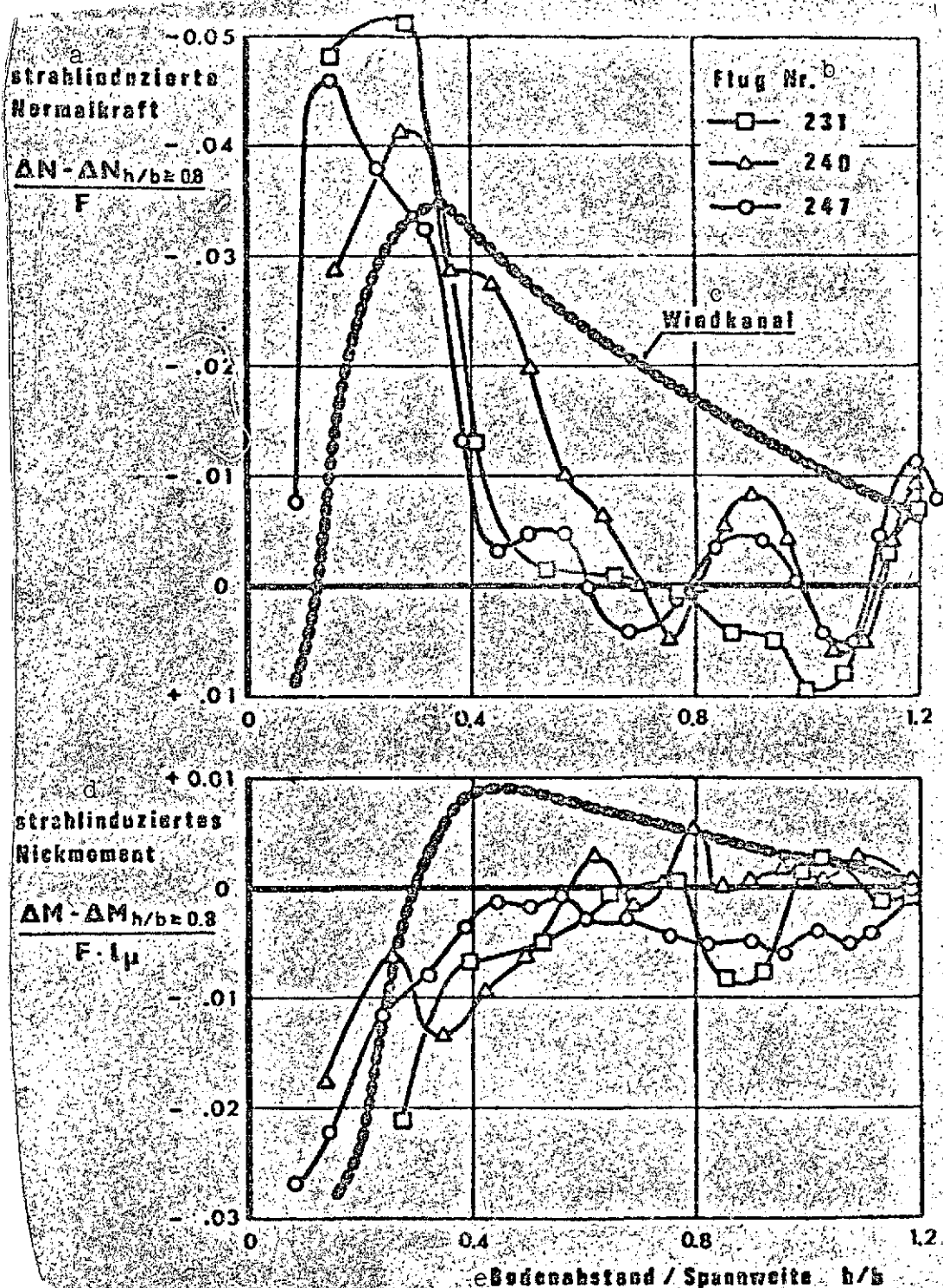


Fig. 9. Jet interference due to ground effect in three Do 31 vertical landings.

Key: a. Jet-induced normal force; b. Flight number; c. Wind tunnel; d. Jet-induced pitching moment; e. Ground distance / wingspan

ORIGINAL PAGE IS
OF POOR QUALITY

$$\frac{-\Delta N}{F}$$

=

K

x

$$\sqrt{\frac{S}{S_a}}$$

x

$$\sqrt{\left(\frac{\partial \frac{q(x)}{P_o - P_\infty}}{\partial \left(\frac{x}{D_a}\right)}\right)_{\max} \times \frac{1}{\left(\frac{x}{D_a}\right)_{\max}}}$$

- strahlind. Normalkraft

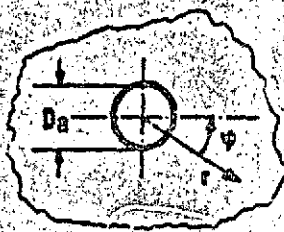
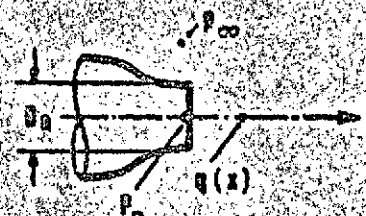
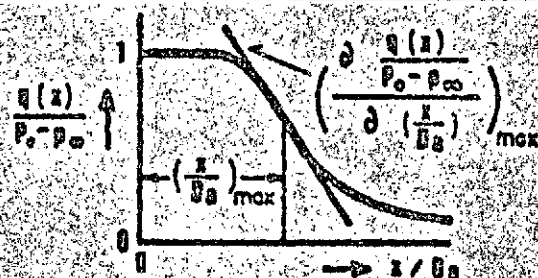
Schub

= Konstante x

$$\sqrt{\frac{\text{Flugzeugfläche}}{\text{Strahlfläche}}}$$

x

$$\sqrt{\frac{\text{max. Staudruckgradient}}{\text{Düsenabstand}}}$$



ANNAHMEN FÜR DIE NACHRECHNUNG DER Do 31

1. $K = 0.009$

2. $\sqrt{\frac{S}{S_a}} = \frac{1}{\pi} \int_0^\pi \left(r(\psi) - \frac{1}{2} D_a \right) d\psi$
(D_a) Einzelstrahl c

3. d Staudruckabnahme des Einzelstrahls

$\left(\frac{-\Delta N}{F}\right)_{\text{Flugzeug}} = \sum \frac{-\Delta N_{\text{Einzelstrahl}}}{F}$		
	f NTW	g NTW
Rechnung h	0.024	0.0336
WT-Messung i	0.022	0.036

Fig. 10. Expression for calculating jet interference in hover.

Key: a. $\frac{-(\text{jet-induced normal force})}{\text{thrust}} = \text{constant} \cdot (\text{aircraft area} / \text{jet area})^{1/2} \cdot (\text{max. stagnation pressure gradient} / \text{nozzle spacing})^{1/2}$; b. Assumptions for Do 31 recalculation; c. Single jet; d. Stagnation pressure dropoff for single jet; e. Aircraft; f. Lift power plant; g. Cruising power plant; h. Calculated; i. Measured in wind tunnel

REFERENCES

1. Gentry, G.L. and Margason, R.J., "Jet-induced lift losses on VTOL configurations hovering in and out of ground effect," NASA TN D-3166, 1966. /14
2. Shumpert, P.K. and Tibbets, J.G., "Model tests of jet-induced lift effects on a VTOL aircraft in hover," NASA CR-1297, 1969.